THE PENNSYLVANIA STATE UNIVERSITY
SCHREYER HONORS COLLEGE

DEPARTMENT OF BIOMEDICAL ENGINEERING

YES-ASSOCIATED PROTEIN 1 LOCALIZATION IN RESPONSE TO SUBSTRATE ARCHITECTURE

COREENA CHAN
SPRING 2019

A thesis
submitted in partial fulfillment
of the requirements
for a baccalaureate degree
in Biology
with honors in Biology

Reviewed and approved* by the following:

Justin Brown
Associate Professor of Biomedical Engineering
Thesis Supervisor

Stephen Schaeffer
Professor of Biology
Associate Head for Graduate Education
Honors Adviser

* Signatures are on file in the Schreyer Honors College.

ABSTRACT

Understanding the interactions between stem cells and their extracellular environment is key to the development of bioscaffolds for tissue regeneration. Yes-associated protein 1 (YAP1) is a transcriptional regulator involved in the Hippo signaling pathway that controls organ size and tumor suppression by regulating cell proliferation and apoptosis. Not much is known about the function of YAP1 in bone homeostasis, but studies have shown evidence that YAP1 promotes osteogenesis and that this mechanism may operate using the FAK/RhoA/YAP1 signaling pathway. In this study, we observed YAP1 nuclear localization in response to unique substrate architectures, including altered cell density and nanofiber surfaces, to reveal the role of YAP1 translocation in specific cell activities, particularly in proliferation and osteogenic differentiation. Culturing mouse mesenchymal stem cells (mMSCs) at greater densities resulted in reduced nuclear localization of YAP1, while lower densities saw increased YAP1 nuclear localization. There was no significant difference in YAP1 nuclear location between mMSCs fixed at similar densities but fixed at different time points, suggesting that YAP1 localization in response to cell density is not temporally controlled. YAP1 nuclear translocation was observed at a specific confluency of mMSCs cultured in increasing stepwise densities, suggesting a possible rapid switch mechanism of YAP1 translocation rather than a gradual translocation process. In altering the surface, human mesenchymal stem cells (hMSCs) cultured on nanofiber surfaces compared to control surfaces demonstrated increased nuclear YAP1 localization. The hMSCs cultured on nanofiber surfaces also demonstrated decreased cell spreading, altered aspect ratios, and larger focal adhesions. Culturing hMSCs on small nanofibers compared to large resulted in greater nuclear YAP1 localization. These data suggest that the formation of larger focal adhesions leads to increased activation of the FAK/RhoA/YAP1 pathway, which results in the translocation of YAP1 to the nucleus to regulate osteogenic differentiation. Understanding the FAK/RhoA/YAP1 pathway through modification of substrate architecture may aid in the development of biomaterials for tissue regeneration.

TABLE OF CONTENTS

LIST OF FIGURES

LIST OF TABLES

ACKNOWLEDGEMENTS

Thank you to Dr. Brown, Dan, Pouria, and Merve for all of their help and patience during my time in the lab, particularly back in the early days when I had no idea what was going on ever. Clearly, this thesis would not exist without all the much-needed support and instruction.

Furthermore, infinite thanks to my lab partner in crime, Ana Hale, without whom we absolutely would not have been able to complete all the experiments we did. I will forever remember every mistake we made (there were a lot) as well as every success that followed.

Chapter 1

Introduction

The regulation of tissue growth and organ size has been a long-standing question in the field of biology. Recently, Yes-associated protein 1 (YAP1) has been studied as potential target for controlling growth, proliferation, and differentiation of various tissues in humans.

YAP1 is a mechanosensitive transcriptional regulator involved in the Hippo signaling pathway that controls organ size and tumor suppression by regulating cell proliferation and apoptosis (Fig. 1) (Das et al., 2016).

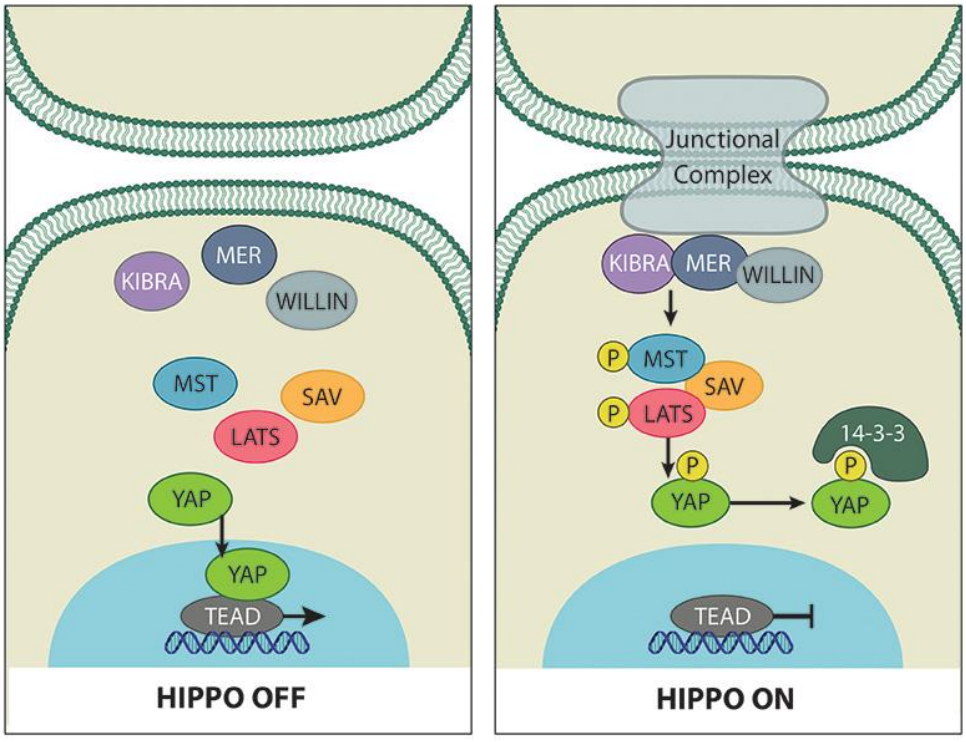

Figure 1 Hippo tumor suppressor pathway that controls the localization of YAP1. (*Source*: National University of Singapore / CC BY-NC 4.0)

Activation of this pathway results in the phosphorylation and inactivation of YAP1 through inhibition of nuclear translocation (Elosegui-Artola et al., 2017). Localization of YAP1 is regulated by a

range of biochemical and mechanical cues, including cell-cell contacts mediated by adherens junction, cell mechano-sensing of extracellular matrix stretch, and soluble factors (Das et al., 2016). Research has shown that mechanical forces from focal adhesions reaching the nucleus reduce nuclear resistance to molecular transport and increase YAP nuclear translocation (Elosegui-Artola et al., 2017).

Previous studies have demonstrated evidence that nuclear YAP1 promotes osteogenesis and that this mechanism may operate using the FAK/RhoA/YAP1 signaling pathway by way of focal adhesions. Focal adhesions are structures created by the clustering of integrins that physically link the actin cytoskeleton to the extracellular matrix (Pirone et al., 2006). Thus, focal adhesions play an important role in the translation of mechanical force to biological signals (Nardone et al., 2017). Focal adhesion kinase (FAK) is a critical effector in focal adhesion signaling that is phosphorylated after clustering of integrins, stimulating its activity through the G-protein RhoA (Pirone et al., 2006). RhoA is a small GTPase protein that senses and responds to mechanical cues by regulating the formation of actin bundles and stress fibers (Zhang et al., 2016). The polymerization of the cytoskeleton in response to mechanical cues from FAK and RhoA transmits signals to the nucleus to regulate gene transcription through YAP1 (Zhang et al., 2016). FAK activation, by phosphorylation of site 397 and 567/577, is believed to decrease RhoA activity and focal adhesion formation (Pirone et al., 2006). Activated RhoA has been found to increase the nuclear translocation of YAP1, whereas the inhibition of RhoA maintains cytoplasmic localization of YAP1 (Zhang et al., 2016). It is not clear if there is a molecular switch mechanism resulting in major shifts of YAP1 localization or if translocation to the nucleus is gradual. Nuclear YAP1 expression is suspected to regulate differentiation through the activity of Runx2, a critical transcription factor involved in osteoblast differentiation (Chang et al., 2018).

Nanofibrous biomaterials have been widely used in the area of tissue regeneration. A major challenge of tissue engineering has been developing scaffolds that are able to imitate the architecture of tissue at the nanoscale but nanofibrous scaffolds have emerged as a potential solution to this challenge (Vasita and Katti, 2006). Recently, nanofibrous architecture has been investigated as a potential substrate

for driving proliferation and osteogenic differentiation in stem cells via FAK/RhoA/YAP1 (Chang et al., 2018). Studies have shown that bone marrow stem cells cultured on nanofibrous architecture demonstrated greater osteogenic differentiation compared to non-nanofibrous architecture (Chang et al., 2018). However, it is not fully understood how nanofibers modulate the FAK/RhoA/YAP1 pathway to control stem cell differentiation.

In this study, we move to determine the temporality of YAP1 translocation and the effects of varied substrate architecture on YAP1 localization, including modifications of cell density and culture surfaces, relative to upstream FAK/RhoA targets. Understanding the regulation of YAP1 translocation by substrate architecture may be the key to constructing extracellular environments that drive specific cell activities, such as cell proliferation and differentiation.

We hypothesize that sub-confluent cells demonstrate increased nuclear localization of YAP1 and that increased confluency of mouse mesenchymal stem cells triggers a molecular switch causing rapid cytoplasmic translocation of YAP1. We will test this hypothesis by seeding mouse mesenchymal stem cells at various densities on a flat surface and observing the localization of YAP1.

We also hypothesize that culturing of human mesenchymal stem cells on nanofibers compared to flat surfaces increase focal adhesion size of cells, decrease FAK phosphorylation at Y576/577, and increase RhoA, leading to increased nuclear localization of YAP1 and increased osteogenic differentiation. Culturing on smaller nanofibers are predicted to amplify these differences. We will test this hypothesis by culturing human mesenchymal stem cells on control flat surfaces and varied nanofiber surfaces, quantifying cell morphologies, nuclear YAP1 localization, and focal adhesions size, and observing trends in osteogenic differentiation via alkaline phosphatase activity.

Chapter 2

Methods

Cell Culture

Cell Density Experiments

Mouse mesenchymal stem cells (mMSCs) were used. Glass cover slips were seeded with between 10,000 cells/cm^2 to 40,000 cells/cm^2 and fixed at 24 hours. Cells were grown in Alpha Minimum Essential Medium (αMEM) supplemented with 10% fetal bovine serum and 1% penicillin streptomycin. Cells were maintained at 37 °C and 5% CO_2.

Nanofiber Experiments

Human mesenchymal stem cells (hMSCs) were used. Control flat surfaces and 3, 6.5, or 10% PMMA nanofiber surfaces were seeded with 5,000 to 10,000 cells/cm^2 and fixed between 24 and 48 hours. Cells were grown in Alpha Minimum Essential Medium (αMEM) supplemented with 10% fetal bovine serum and 1% penicillin streptomycin. Cells were maintained at 37 °C and 5% CO_2.

Electrospinning

Poly(methyl methacrylate) nanofibrous substrates were prepared via electrospinning with a stationary copper target, chosen for its high conductivity. PMMA was dissolved in a 3:1 dimethylformamide : tetrahydrofuran solution at 25% w/v and transferred to a 5 mL glass syringe with a 25G needle. The syringe was placed a syringe pump with a 6 mL h”1 flow rate and a 10kV voltage was

applied between the syringe tip and copper target. Fibers were collected on glass coverslips located 18 cm from the syringe needle tip, previously coated with 2% w/v poly(2-hydroxyethyl methacrylate) (PHEMA) dissolved in 70% ethanol through spincoating at 5000 rpm for 10 seconds. PHEMA prevents the adhesion of cells to the glass coverslip. The fiber-deposited slides were then heated twice on a 120 1C hot plate for 1 min each and sterilized with UV treatment before experimentation.

Flat Surface Preparation

Control flat surfaces were prepared used 22 mm^2 glass cover slips. Poly(methyl methacrylate) (PMMA) was dissolved in nitromethane overnight at 32°C to create a 4% solution. Glass coverslips were soaked in KOH solution overnight, washed with isopropanol and deionized water, and coated in the 4% PMMA solution through spincoating at 5000 rpm for 10 seconds.

Immunofluorescence Staining

Mouse or human mesenchymal stem cells were fixed with 10% paraformaldehyde in 1x phospho-buffered saline (PBS, NaCl, KCl, Na_2HPO_4, KH_2PO_4) for 15 minutes, washed with cytoskeleton stabilization buffer (CSB, NaCl, piperazine-N,N′-bis(2-ethanesulfonic acid), $MgCl_2$, EGTA, sucrose, 0.5% Triton X-100), and washed (3 x PBS). After cells were blocked with permeabilization buffer (2% bovine serum albumin and 0.1% Triton X-100 in 1xPBS) for 45 minutes at room temperature, they were stained with anti-vinculin antibody (1:400), anti-YAP1 antibody (1:500), or anti-integrin beta 5 (1:400) for 1 hour at room temperature. Then, the cells were stained with Alexa Fluor secondary antibody (1:400) for 45 minutes, followed by Alexa Fluor phalloidin (1:1500) and DAPI (1:1000) for 30 minutes, in the dark at room temperature. Vinculin and integrin beta 5 are markers for focal adhesions, since vinculin is a membrane cytoskeletal focal adhesion protein and integrin beta 5 is a transmembrane integrin adhesion

molecule linked to focal adhesions. The glass cover slips were mounted, sealed with clear nail polish, and observed under a confocal laser scan microscope.

Alkaline Phosphatase Detection

Mouse or human mesenchymal stem cells grown on control flat or nanofiber surfaces were lysed with Mammalian Extraction Reagent (M-PER) and subject to one freeze-thaw cycle. Samples were incubated in p-nitrophenol phosphate solution for 30 minutes and osteogenic differentiation was quantified via absorbance. Data was normalized to fluorescence values obtained from a PicoGreen dsDNA Assay.

Statistical Analysis

Quantitative data from images were analyzed using CellProfiler and ImageJ software, including cell area, circularity index, aspect ratio, fluorescence intensity, nuclear area, and focal adhesion size. Data were analyzed with t-test with a statistical significance set at $p < 0.05$. For confluency experiments, seeding conditions were compared between one another (i.e. 10K vs. 20K cells/cm^2) using data averaged from 10-20 images per condition. For nanofiber and ALP experiments, nanofiber slides were compared to control slides using data averaged from 40-50 images per condition. Data for every experimental condition was averaged from 2-3 replicate slides.

Chapter 3

Results and Discussion

Cell Density Experiments

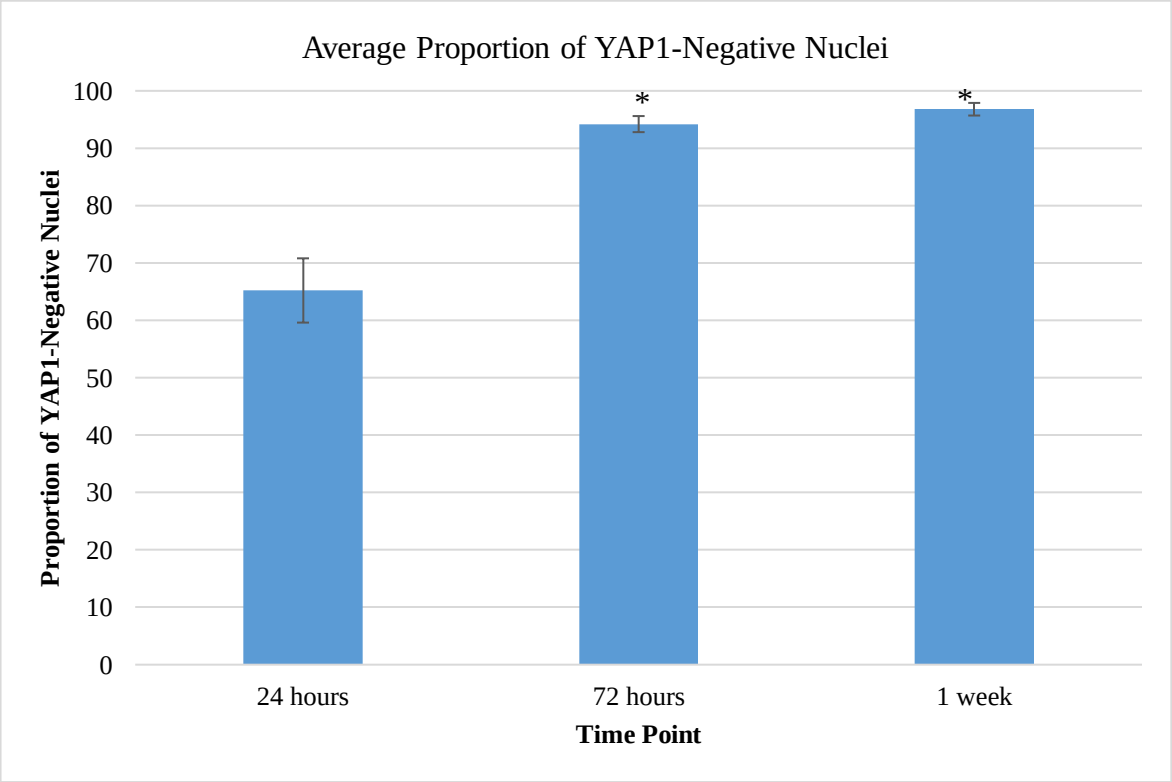

Figure 2 Average proportion of YAP1-negative nuclei in mMSCs fixed at 1-, 3-, and 7-day time points. * indicates $p < 0.05$ compared with 24-hour time point.

In this experiment, glass cover slips were prepared with an initial seeding density of 10,000 cells/cm^2. YAP1-positive nuclei were identified as white-appearing nuclei due to the presence of green YAP1 fluorescence overlapping purple nuclei fluorescence. Therefore, greater YAP1-positive nuclei would indicate greater nuclear YAP1 localization, whereas greater YAP1-negative nuclei indicates greater cytoplasmic localization. The mMSCs fixed at 24 hours (Fig. 3) contained a lower proportion of YAP1-

negative nuclei, indicating that mMSCs fixed at 24 hours exhibited decreased cytoplasmic YAP1 localization compared to cells fixed at 72 hours (Fig. 4) and 1 week (Fig. 5) (Fig. 2). The mMSCs fixed at 72 hours and 1 week also demonstrated a greater cell density compared to the 24-hour time point. As predicted by our hypothesis, sub-confluent cells exhibited greater nuclear YAP1 localization and thus increased YAP1 activation due to reduced cell-cell contact inhibition. Cell density has been shown to regulate YAP1 nuclear localization to modulate cell proliferation (Das et al., 2016). This cell-cell contact inhibition occurs via the Hippo pathway, in which the Lats tumor supressor kinase causes cytoplasmic translocation and therefore inactvation of YAP1 (Zhao et al., 2007).

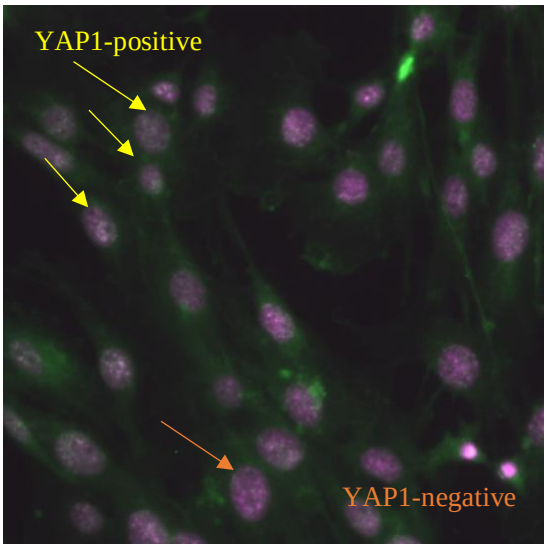

Figure 3 YAP1 fluorescence (green) and nuclei (purple) in mMSCs fixed at 24 hours**.**

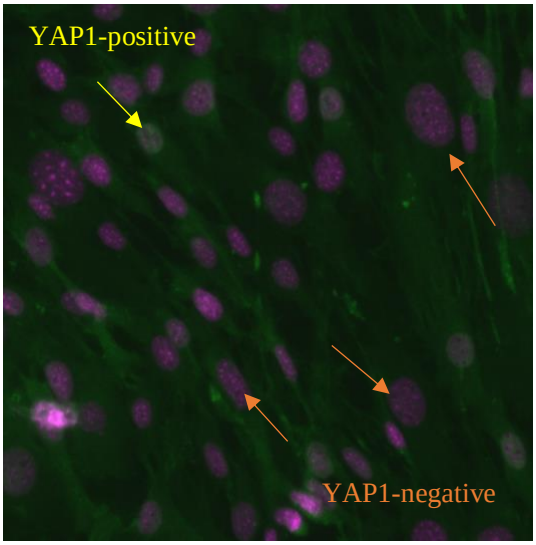

Figure 4 YAP1 fluorescence (green) and nuclei (purple) in mMSCs fixed at 72 hours.

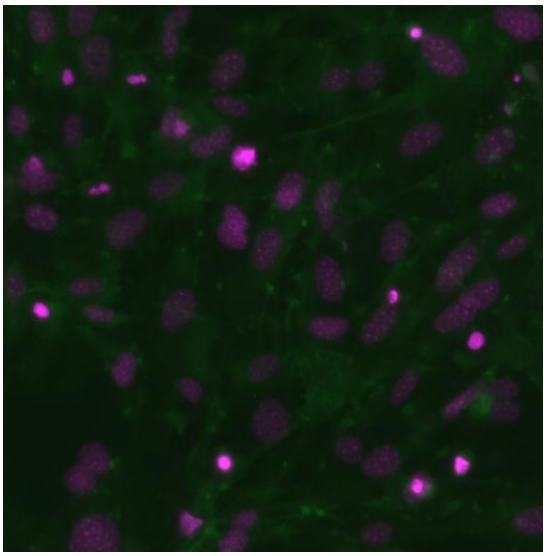

Figure 5 YAP1 fluorescence (green) and nuclei (purple) in mMSCs stained at 1 week.

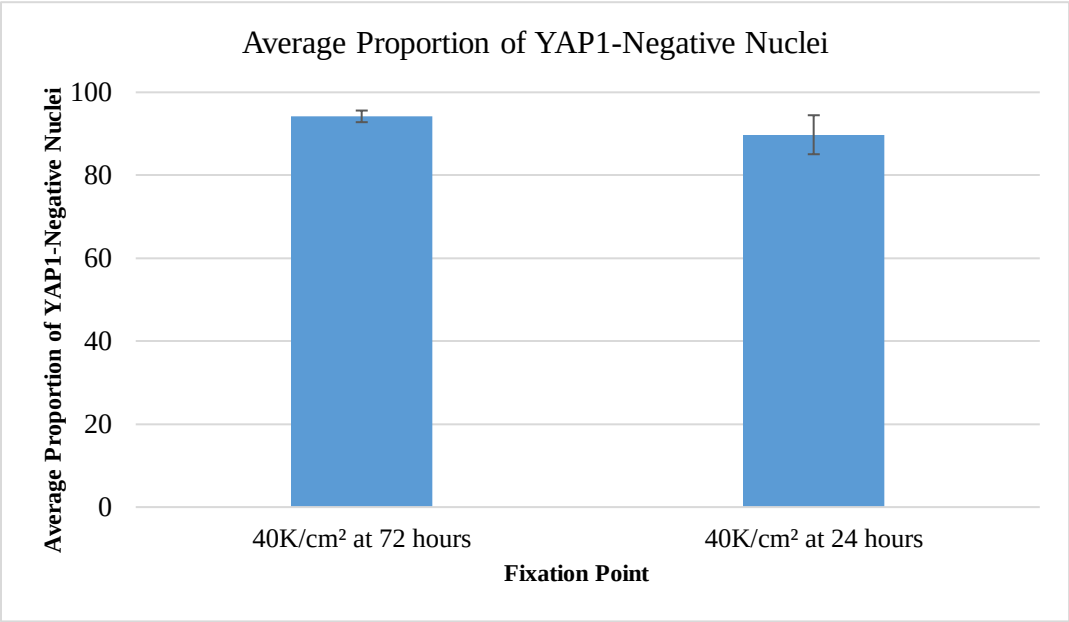

Figure 6 Average proportion of YAP1-negative nuclei in mMSCs fixed at 72 hours with cell density of approx. 40,000 cells/cm^2 and at 24 hours with cell density of approx. 40,000 cells/cm^2.

In following experiments, mMSCs were seeded at varied initial cell densities and fixed at 24 hours to allow adherence but minimize proliferation (Fig. 8-13). There was no observable difference in YAP1 nuclear localization between mMSCs seeded at 10,000 cells/cm^2 and fixed at 72 hours with a

density of approximately 40,000 cells/cm^2 compared to mMSCs seeded at 40,0000 cells/cm^2 and fixed at 24 hours (Fig. 6). These data suggest that YAP1 nuclear translocation in response to cell density is not temporally controlled but instead determined by cell confluency.

Cells were seeded incrementally between 10,000 and 40,000 cells/cm^2 and observed for YAP1 localization. As predicted, increasing seeding density appeared to correlate with decreasing nuclear YAP1 localization (Fig. 7). YAP1 nuclear localization was observed to significantly differ between mMSCs seeded at 25,000 and 30,000 cells/cm^2 but not between densities below 25,000 or between densities above 30,000 cells/cm^2. These data suggest a possible YAP1 switch mechanism as hypothesized, specifically when cell density reaches a threshold between 25,000 and 30,000 cells/cm^2. In response to the accumulation of cell-cell contacts at this particular density, YAP1 may undergo rapid cytoplasmic translocation to inhibit further proliferation.

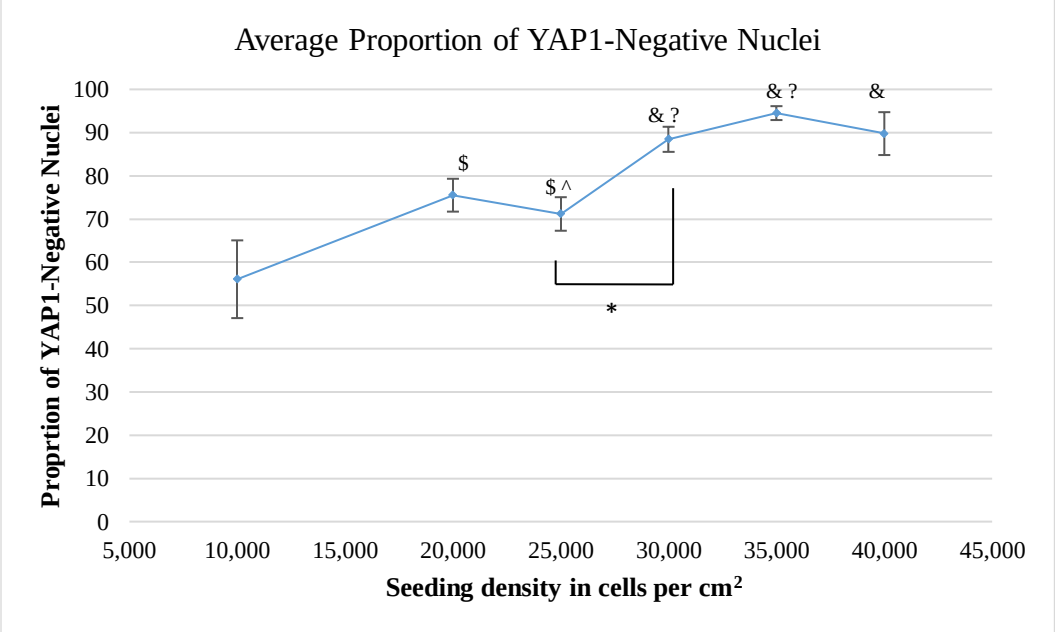

Figure 7 Average proportion of YAP1-negative nuclei by seeding cell density. * indicates a $p < 0.05$. & indicates $p < 0.05$ compared to 10,000 cells/cm^2. ? indicates $p < 0.05$ compared to 20,000 cells/cm^2. ^ indicates $p < 0.05$ compared to 35,000 cells/cm^2. $ indicates $p < 0.05$ compared to 40,000 cells/cm^2.

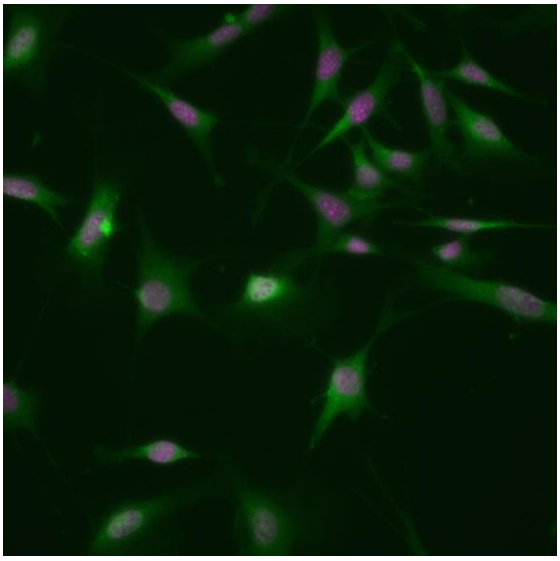

Figure 8 YAP1 fluorescence (green) in mMSCs seeded at 10,000 cells per cm^2.

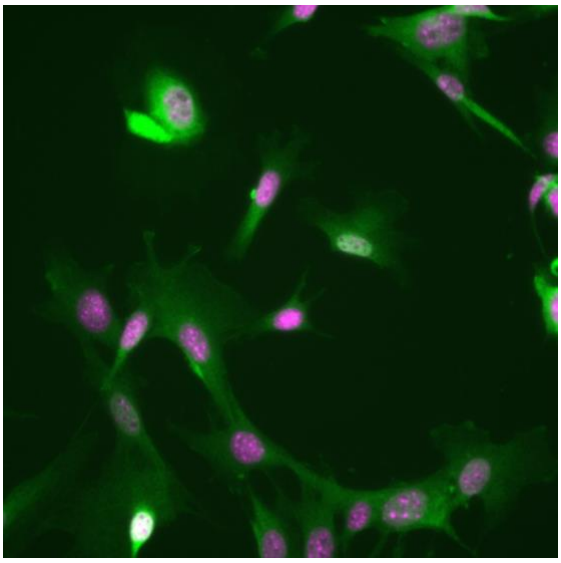

Figure 9 YAP1 fluorescence (green) in mMSCs seeded at 20,000 cells per cm^2.

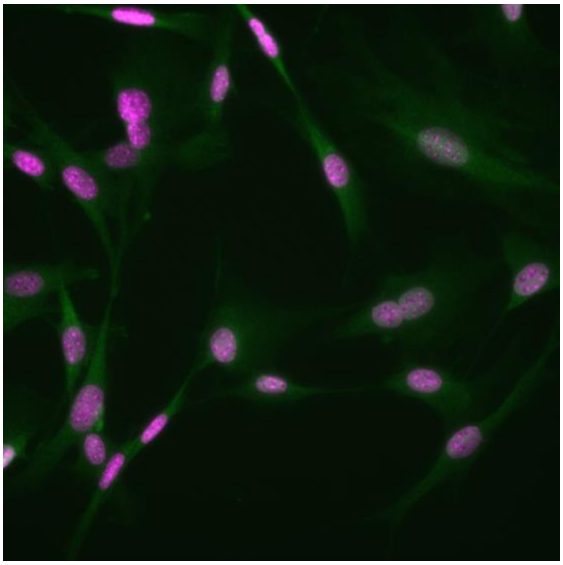

Figure 10 YAP1 fluorescence (green) in mMSCs seeded at 25,000 cells per cm^2.

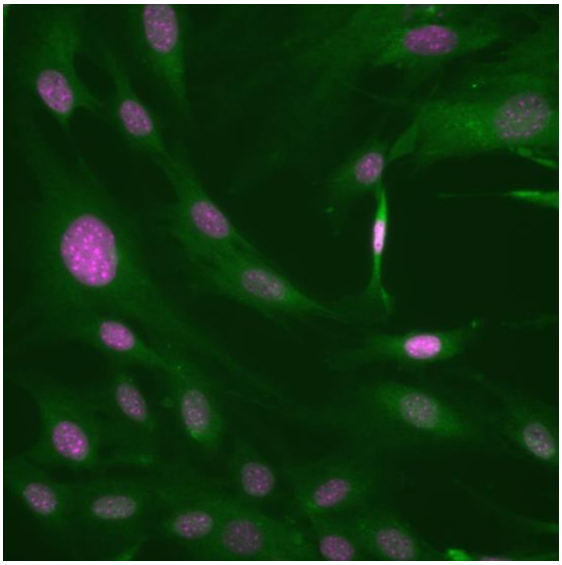

Figure 11 YAP1 fluorescence (green) in mMSCs seeded at 30,000 cells per cm^2.

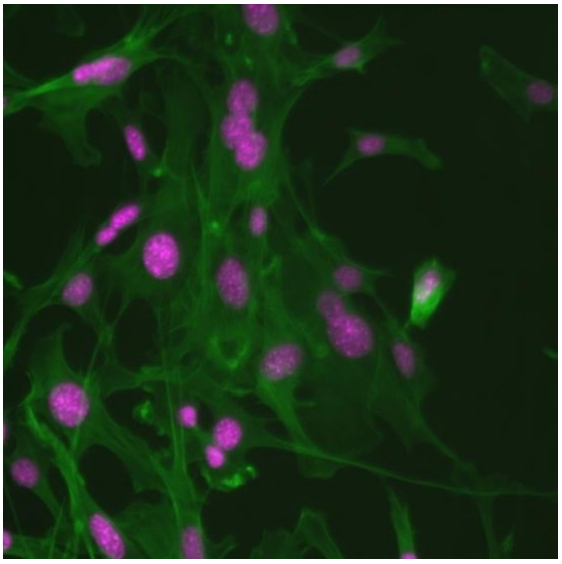

Figure 12 YAP1 fluorescence (green) in mMSCs seeded at 35,000 cells per cm^2.

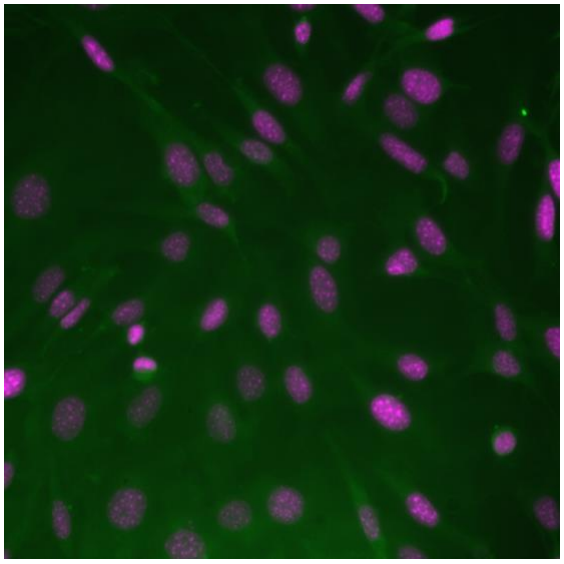

Figure 13 YAP1 fluorescence (green) in mMSCs seeded at 40,000 cells per cm^2.

Nanofiber Experiments

In these experiments, hMSCs were seeded on PMMA control flat surfaces or PMMA nanofibers. The thickness of nanofibers was determined by the concentration of PMMA in solution used for electrospinning (Piperno et al., 2006). In these experiments, small nanofibers (3% PMMA) (Fig. 14), medium nanofibers (6.5% PMMA) (Fig.15), and large nanofibers (10% PMMA) (Fig. 16) were used. Cells were seeded at a density between 5,000 to 10,000 cells/cm^2 and fixed between 24 and 48 hours.

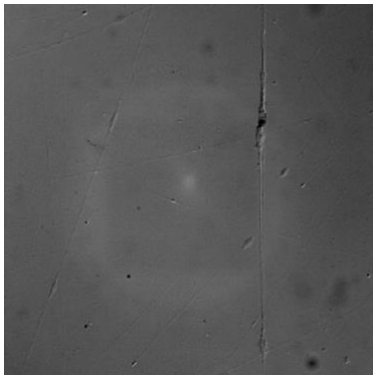

Figure 14 Small (3% PMMA) nanofibers.

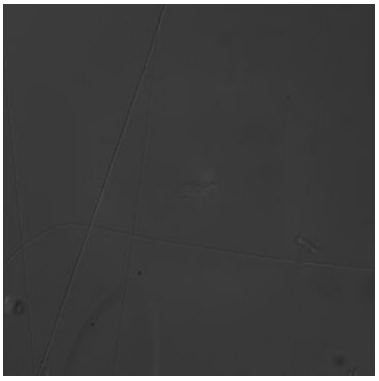

Figure 15 Medium (6.5% PMMA) nanofibers.

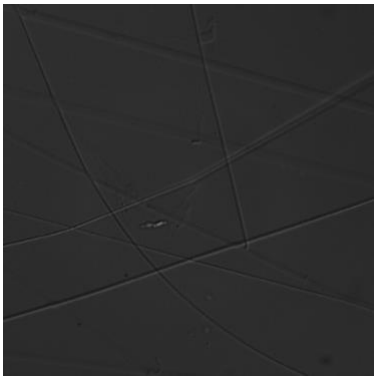

Figure 16 Large (10% PMMA) nanofibers.

Experiment 1 – Cell morphologies and nuclear YAP1 on 10% PMMA nanofibers

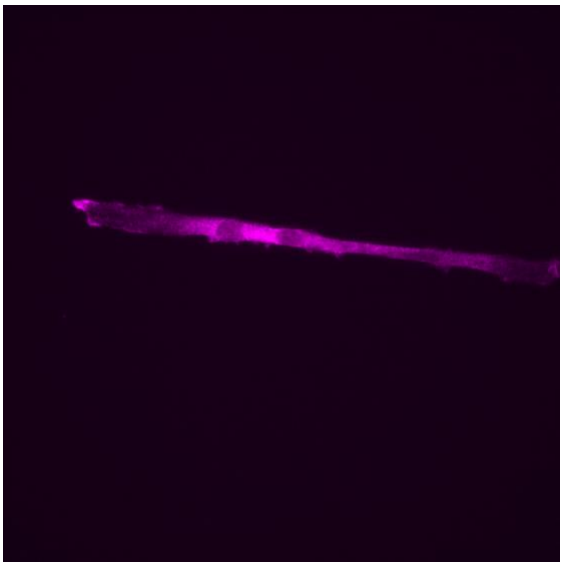

Figure 17 YAP1 fluorescence (pink) of hMSCs seeded on 10% PMMA nanofibers.

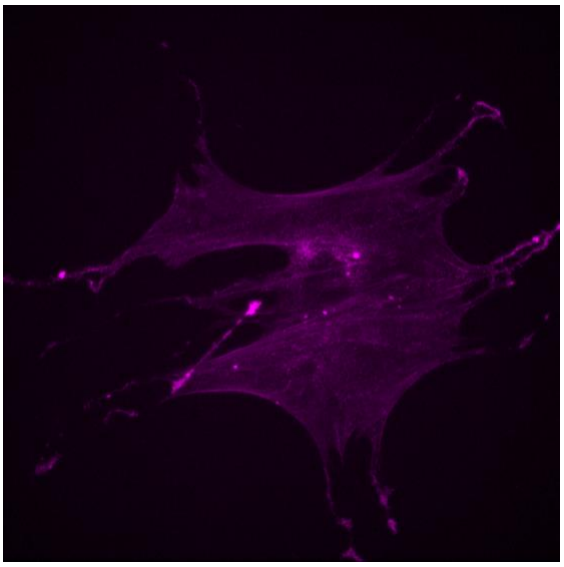

Figure 18 YAP1 fluorescence (pink) of hMSCs seeded on a PMMA control flat surface.

Cell Morphology

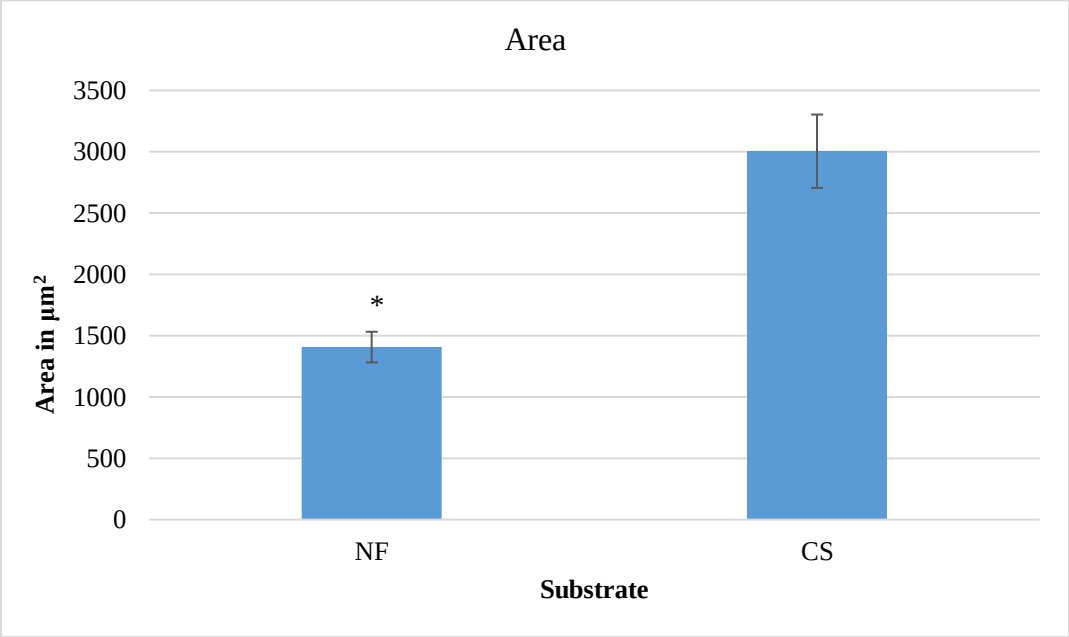

Figure 19 Average cell area of hMSCs seeded on 10% PMMA nanofibers or a PMMA control flat surface. * indicates $p < 0.05$ compared to control.

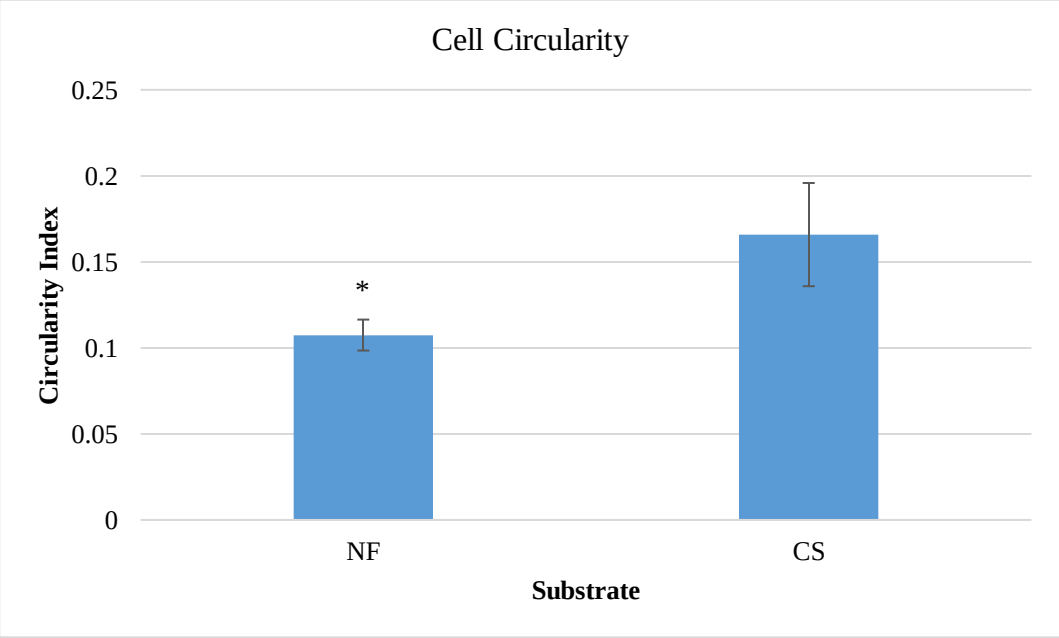

Figure 20 Average circularity index of hMSCs seeded on 10% PMMA nanofibers or a PMMA control flat surface. * indicates $p < 0.05$ compared to control.

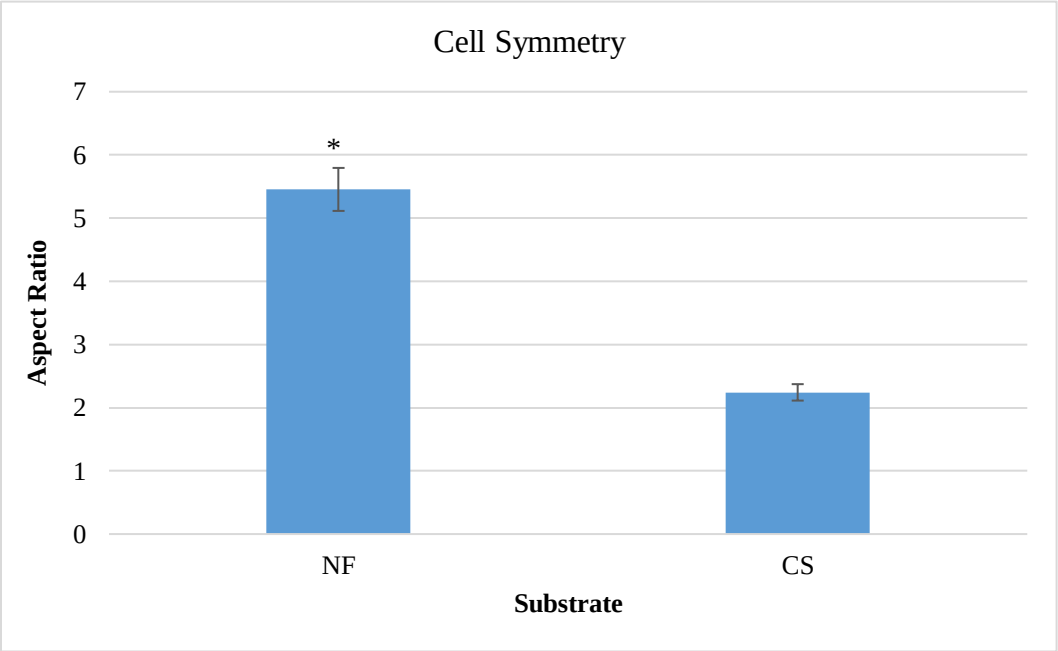

Figure 21 Average aspect ratio of hMSCs seeded on 10% PMMA nanofibers or a PMMA control flat surface. * indicates $p < 0.05$ compared to control.

Cell morphologies of hMSCs were quantified by two indices: the circularity index ($CI=4\pi A/L^2$) and aspect ratio (AR). The circularity index is a measure of the circularity of a cell, where A is the area of the cell and L is the perimeter. Aspect ratio is a measure of symmetry, and is the ratio of the major cell axis length to the minor cell axis length. CI=1 represents a perfect circle and AR=1 represents absolute symmetry. In this experiment, hMSCs seeded on PMMA control flat surfaces on average had a larger area (3004.48 vs 1407.11 μm^2), greater circularity index (0.17 vs 0.11), and smaller aspect ratio value (2.2 vs 5.5). The hMSCs cultured on PMMA control flat surfaces (Fig. 17) exhibited more spreading and extension of cellular processes compared to those cultured on 10% PMMA nanofibers (Fig. 18), which appeared more oblong and less cellular processes. Cells adhered to nanofibers appeared to elongate along fiber axes. According to other studies, nanofibrous architecture is believed to modulate stem cells to form an in-vivo-like morphology (Chang et al., 2018).

Nuclear YAP1 Localization

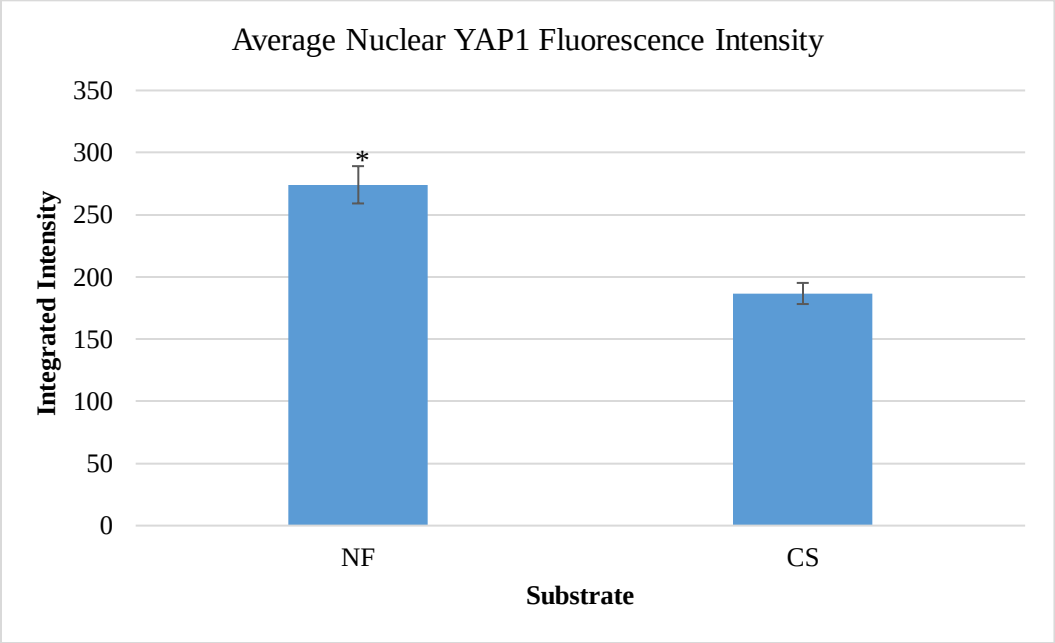

Figure 22 Average nuclear YAP1 fluorescence intensity of hMSCs seeded on 10% PMMA nanofibers or a PMMA control flat surface. * indicates $p < 0.05$ compared to control.

Nuclear localization of YAP1 was quantified by measuring an intensity value of YAP1 fluorescence. The hMSCs cultured on 10% PMMA nanofibers demonstrated significantly greater nuclear YAP1 localization (274 vs 186 intensity value), which supports our hypothesis. A potential mechanism for this process is mechanical transduction through the extracellular matrix. Research has shown that cytoskeletal tension that occurs at the cell surface is transmitted to the nuclear envelope, creating nuclear strain. Force transmission to the nucleus results in a RhoA-dependent translocation and activation of YAP1 (Driscoll et al. 2015). In the nucleus, YAP1 regulates gene transcription to control proliferation and differentiation.

Experiment 2 – Cell morphologies and focal adhesion size on 10% PMMA nanofibers

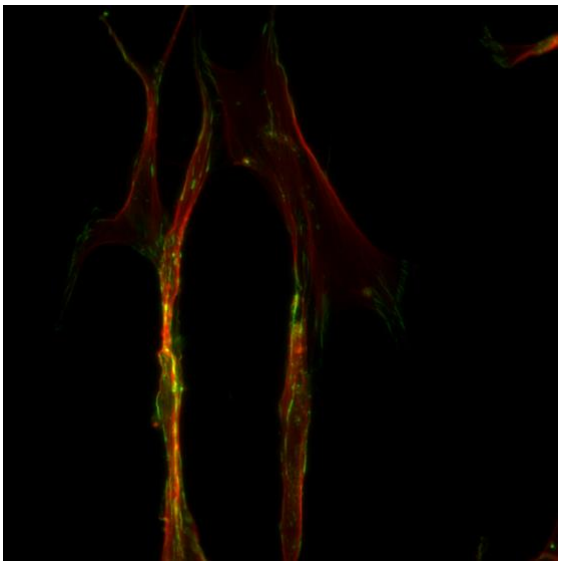

Figure 23 Focal adhesion fluorescence (green) of hMSCs seeded on 10% PMMA nanofibers.

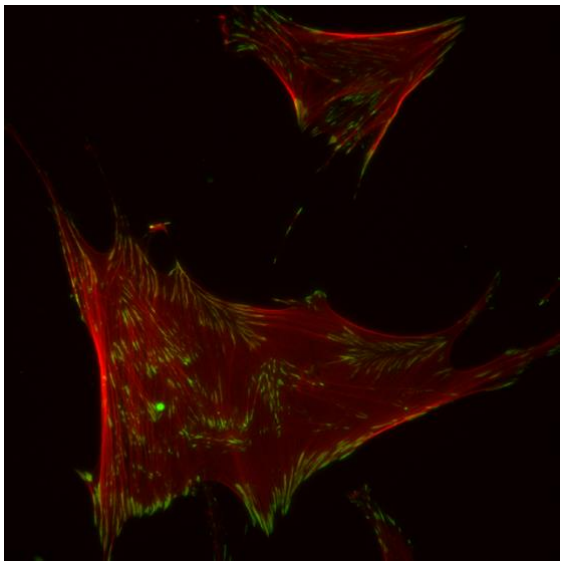

Figure 24 Focal adhesion fluorescence (green) of hMSCs seeded on a PMMA control flat surface.

Cell Morphology

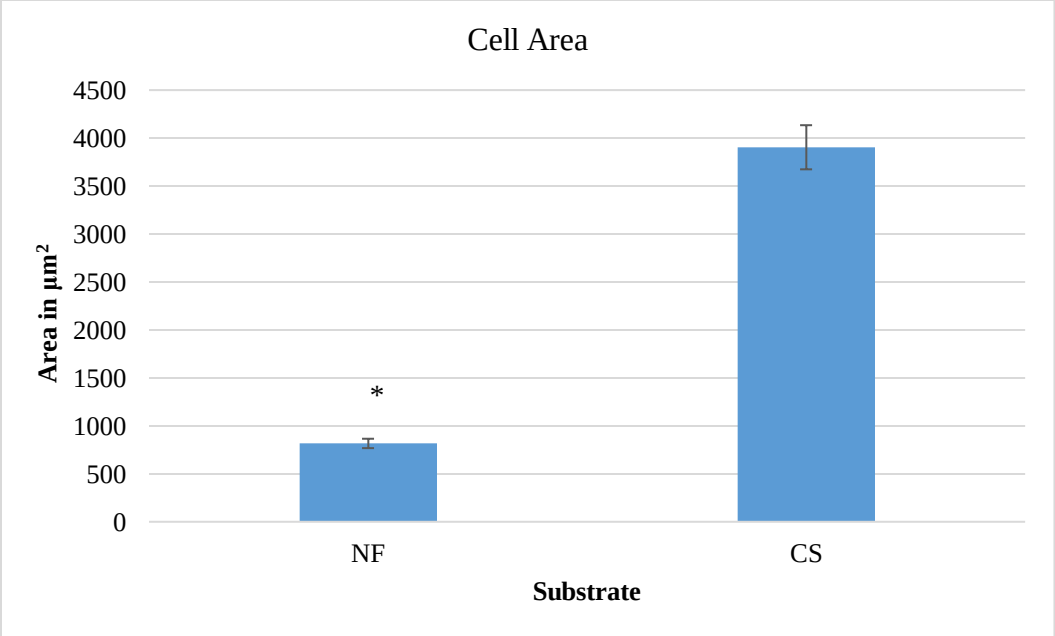

Figure 25 Average cell area of hMSCs seeded on 10% PMMA nanofibers or a PMMA control surface. * indicates $p < 0.05$ compared to control.

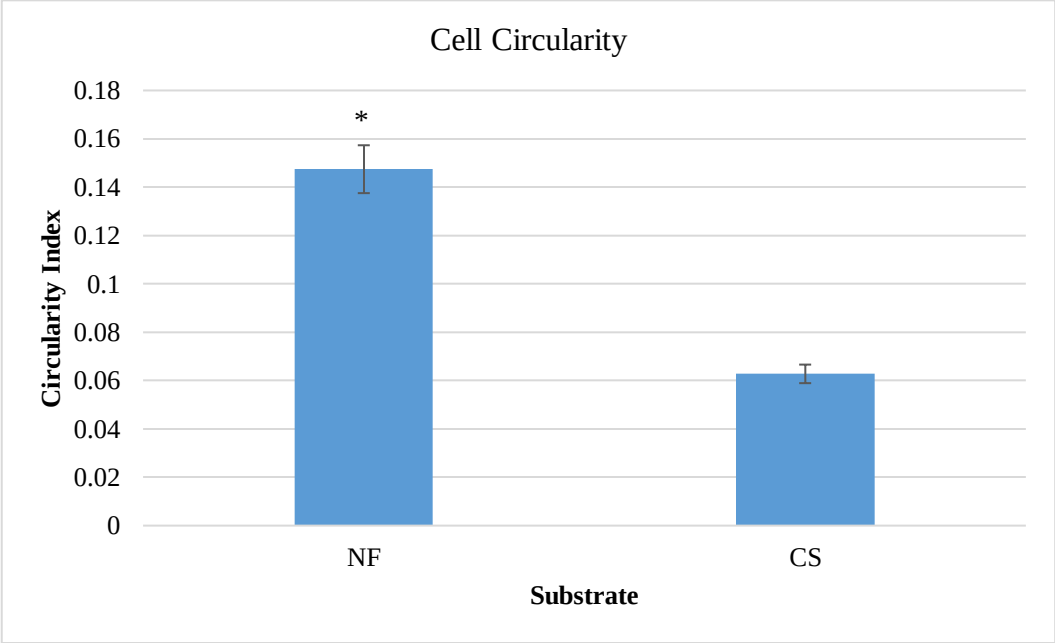

Figure 26 Average circularity index of hMSCs seeded on 10% PMMA nanofibers or a PMMA control surface. * indicates $p < 0.05$ compared to control.

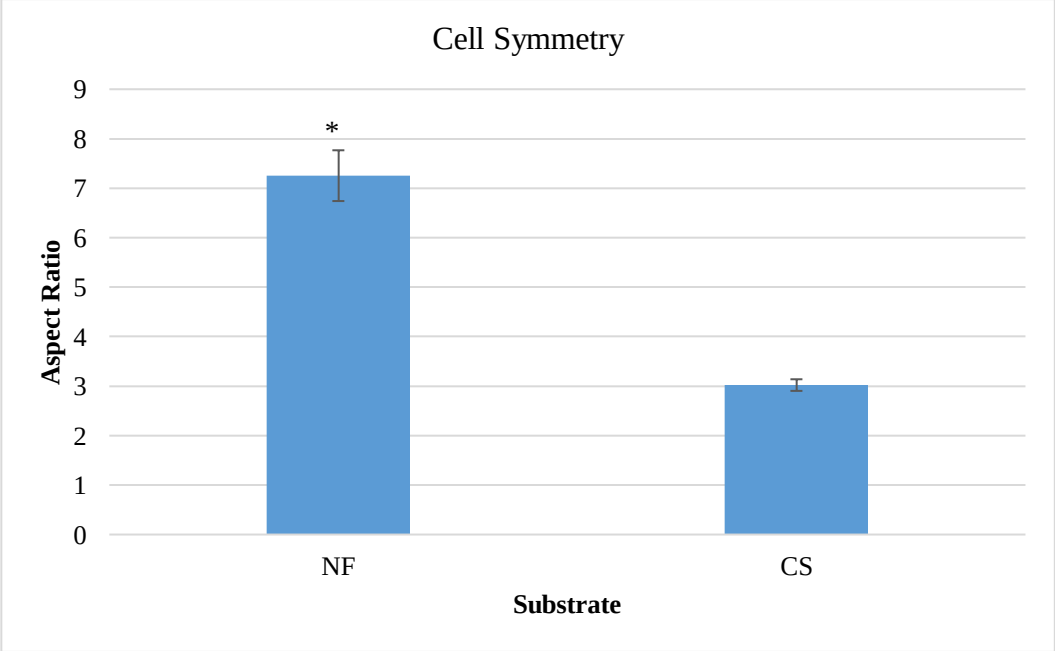

Figure 27 Average aspect ratio of hMSCs seeded on 10% PMMA nanofibers or a PMMA control surface. * indicates $p < 0.05$ compared to control.

In this experiment, hMSCs seeded on PMMA control flat surfaces on average had a larger area (3904.01 vs 816.76 μm^2), smaller circularity index (0.6 vs 0.15), and a smaller aspect ratio value (3.02 vs 7.25). Though conditions were the same, these results were not consistent with the results of the previous experiment. However, images of the hMSCs on PMMA control flat surface still did demonstrate greater spreading compared to the more narrow-shaped cells cultured on 10% PMMA nanofibers. These conflicting results may be explained by a notable number of hMSCs cultured on nanofiber surfaces that did adhere to the nanofibers themselves. Regardless, it is not clear which substrate results in the formation of more in-vivo-like cell morphology.

Focal Adhesions

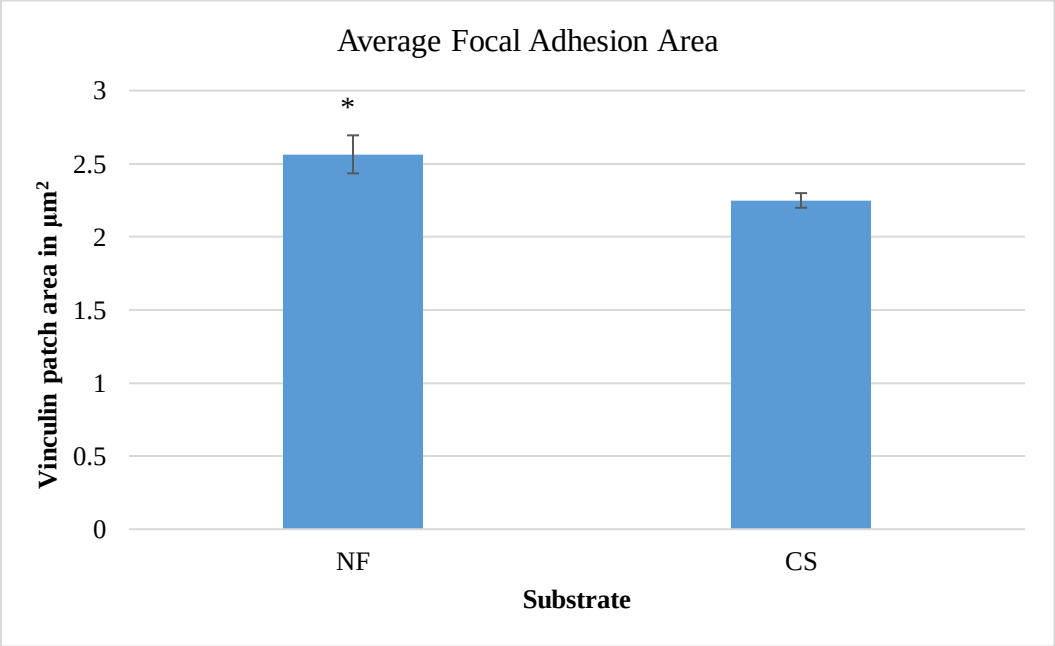

Figure 28 Average focal adhesion area of hMSCs seeded on 10% PMMA nanofibers or a PMMA control flat surface. * indicates $p < 0.05$ compared to control.

Focal adhesions act as a bridge between actin fibers and extracellular integrins. Mature focal adhesions are linear vinculin patches associated with the termini and stress fibers (Chang et al., 2018). Average focal adhesion size of hMSCs were quantified by the area of the individual vinculin patches. The

hMSCs cultured on 10% PMMA nanofibers compared to PMMA control flat surfaces demonstrated formation of larger focal adhesions (2.56 vs 2.25), which supports our hypothesis. Focal adhesions appeared more distributed on cells seeded on control surfaces (Fig. 23), whereas those on nanofiber surfaces appeared more clustered (Fig. 22). These results are similar previous studies on C2C12 cells grown on polystyrene nanofiber scaffolds, which demonstrated formation of longer and more concentrated focal adhesion complex clusters compared to flat control surfaces (Sheets et al., 2013). Nanofibrous architecture is believed to provide a more in-vivo-like environment for stem cell adhesion than smooth surfaces (Chang et al., 2018).

Experiment 3 – Nuclear YAP1 on small, medium, and large fibers

The hMSCs cultured on PMMA control flat surfaces (Fig. 28) demonstrated greater spreading compared to hMSCs cultured on small, medium, and large nanofibers. Regardless of the size of nanofiber, the hMSCs grown on nanofibers appeared narrower in contrast to the more spread out cells on control surfaces. Cells seeded on slides with small nanofibers appeared to adhere less to the fibers compared to the medium and large nanofibers.

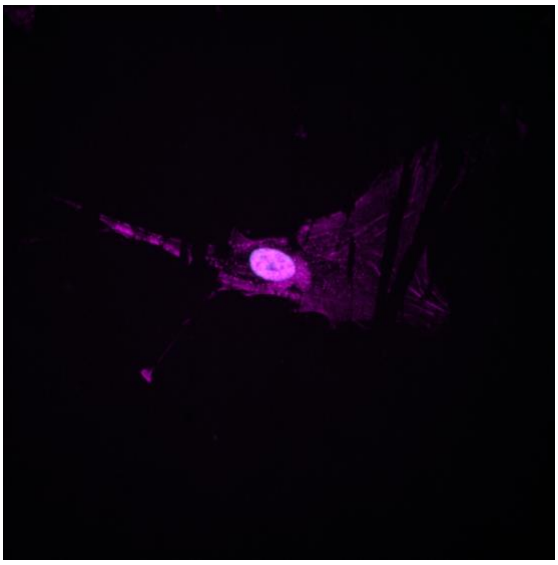

Figure 29 YAP1 fluorescence (pink) of hMSCs seeded on a PMMA control flat surface.

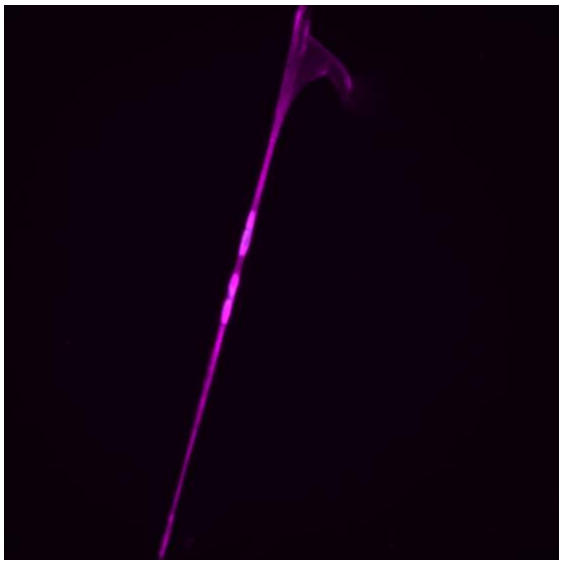

Figure 30 YAP1 fluorescence (pink) of hMSCs seeded on small nanofibers.

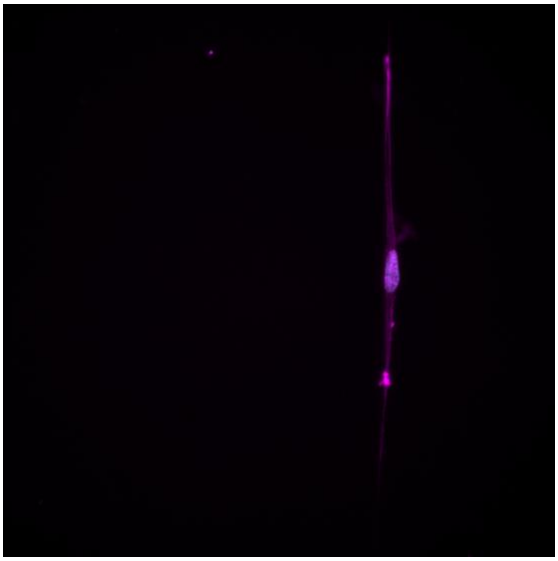

Figure 31 YAP1 fluorescence (pink) of hMSCs seeded on medium nanofibers.

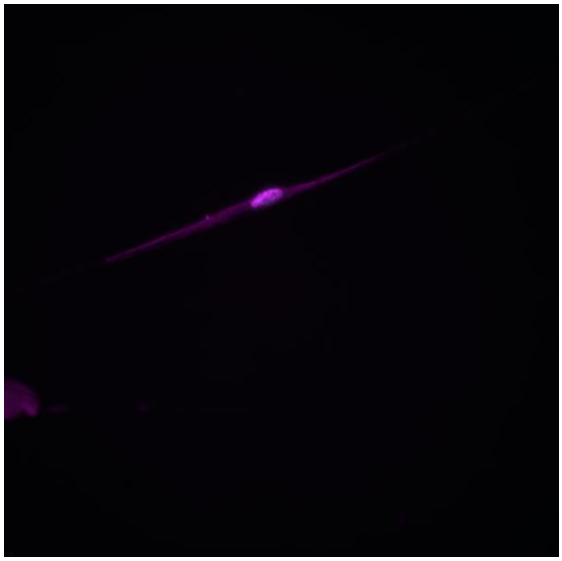

Figure 32 YAP1 fluorescence (pink) of hMSCs seeded on large nanofibers.

Nuclear YAP1

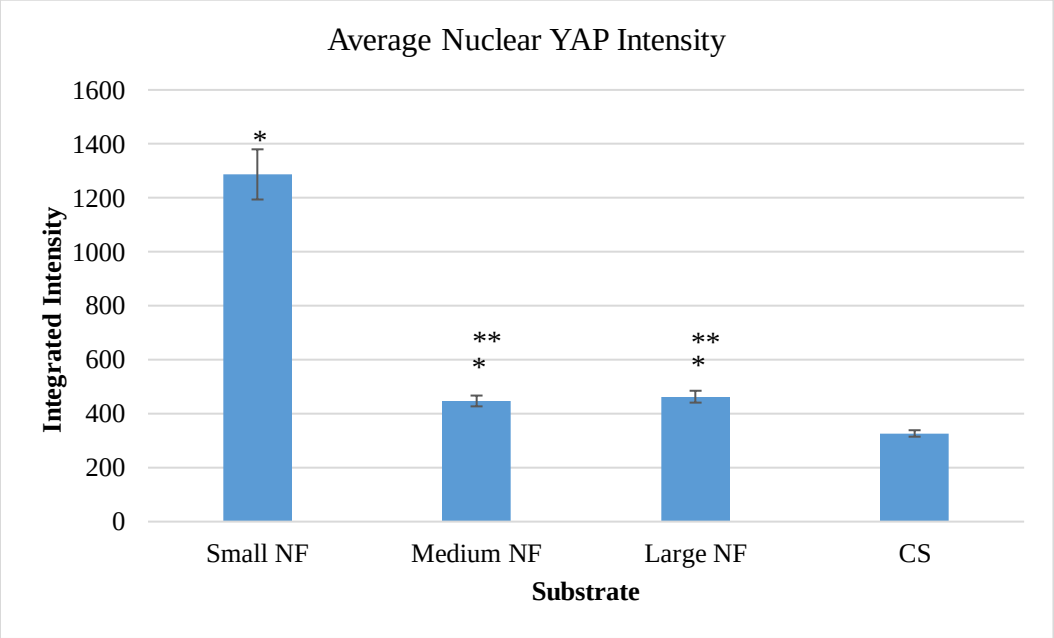

Figure 33 Average nuclear YAP1 fluorescence intensity of hMSCs seeded on small, medium, or large nanofibers or a PMMA control flat surface. * indicates $p < 0.05$ compared to control. ** indicates $p < 0.05$ compared to small nanofibers.

The hMSCs cultured on small nanofibers demonstrated greater YAP1 fluorescence intensity compared to all other substrates (1286.9) (Fig. 32), while the hMSCs cultured on PMMA control flat surfaces demonstrated a smaller YAP1 fluorescence intensity value compared to all other substrates (326.7). As hypothesized, culturing of hMSCs on smaller nanofibers resulted in greater nuclear YAP1 localization compared to control surfaces and larger nanofibers. However, hMSCs cultured on medium nanofibers compared to large nanofibers did not significantly differ, suggesting that the diminution in size from large to medium fibers was not sufficient to affect YAP1 localization. It is possible that the small nanofibers resulted in the formation of larger focal adhesions, but vinculin patches were unable to be quantified due to the compactness of cells adhered to the small nanofibers.

ALP Experiments

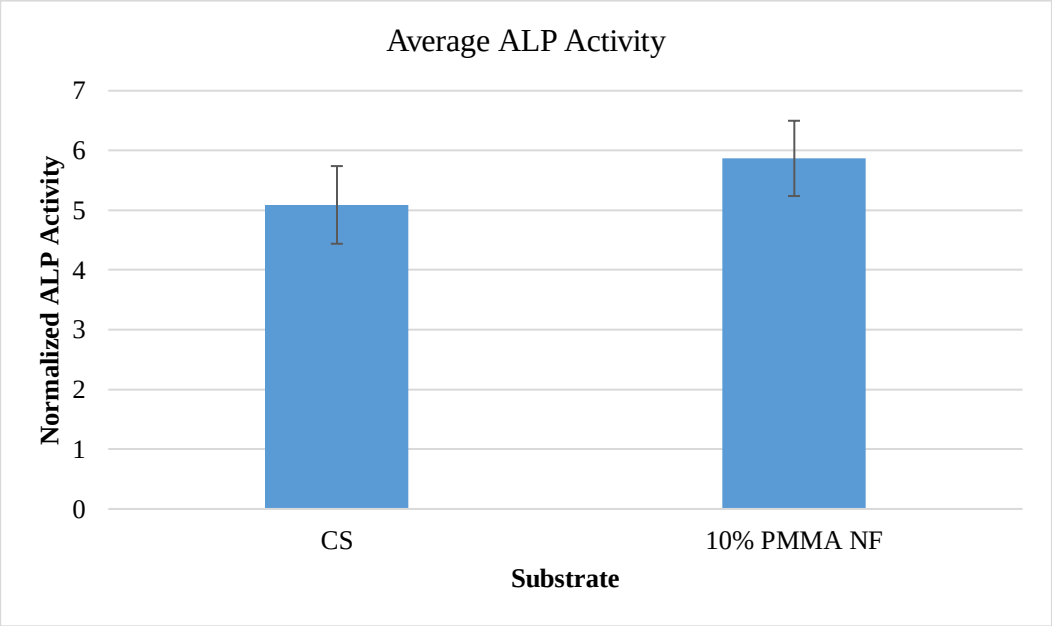

Figure 34 ALP activity of hMSCs seeded on 10% PMMA nanofibers or a PMMA control flat surface and incubated for 48 hours.

In this experiment, hMSCs were seeded on 10% PMMA nanofibers and control flat surfaces and incubated for 48 hours. There was no difference in osteogenic differentiation between hMSCs grown on PMMA control flat surfaces and 10% PMMA nanofibers (Fig. 34). These results do not support our hypothesis. It is possible that the cells were not incubated on the substrates long enough to derive any effect on osteogenic differentiation. A differentiation medium was also not used. Other similar studies have demonstrated that nanofibrous architecture enhances osteogenic differentiation of stem cells (Chang et al., 2018).

Challenges

Throughout the course of this project, several issues were encountered while conducting particular experiments that resulted in a few experiments that were not completed before the thesis deadline. There was particular difficulty in capturing data concerning FAK phosphorylation and osteogenic differentiation.

We attempted two methods of quantifying FAK activity at site 576/577, including immunofluorescence staining and the western blot. Immunofluorescence staining FAK did not yield any usable data due to the presence of background noise while imaging, which prevented the accurate identification of FAK fluorescence. A next attempt at this experiment might be improved by using different secondary antibodies or both FAK and f-actin. Western blotting was attempted in addition to immunostaining because data on FAK concentration was expected to be more informative than FAK fluorescence. Regardless, 5 western blots and several spotting tests were attempted without success. While the scans on the Licor Odyssey revealed effective transfers of the protein ladder, no bands were observed for any of the samples probed for FAK or other specific proteins, although a total protein stain was successful. In a second western blot probing for FAK specifically, we added phosphatase inhibitors to the lysis buffer and PBS wash to counteract FAK dephosphorylation at site 576/577 but results did not change.

To quantify osteogenic differentiation of hMSCs grown on nanofibers and control flat surfaces, cells were cultured on these substrates and then measured for alkaline phosphatase activity. In these experiments, the main complication was identifying the optimal duration for which the cells should remain on the substrates before lysis. Data was obtained for ALP activity of hMSCs incubated for 48 hours (Fig. 33), 5 days, and 10 days, but these results were not consistent and inconclusive. There was also some suspicion that the samples were either dilute or too briefly incubated in ALP to sufficiently complete the reaction before analysis of absorbance.

While conducting the cell density experiments, the primary issue encountered was the method of quantifying nuclear vs cytoplasmic YAP1 localization. The method selected was binary identification of either YAP1-negative or positive nuclei based examination of color. YAP1-positive nuclei would appear

white due to the mixing for green YAP1 fluorescence with the purple nuclear fluorescence, indicating presence of YAP1 in the nucleus. YAP1-negative nuclei would appear purple due to the absence of green YAP1 fluorescence and thus YAP1 in the nuclei. This method of subjectively identifying color was revealed to be too imprecise to provide reliable data. This issue was particularly noted when replicate experiments provided contradictory data. For instance, replicate experiments revealed significantly different values for mMSCs seeded at the same density, such as those seeded at 20,000 cells/cm^2 (Fig. 35).

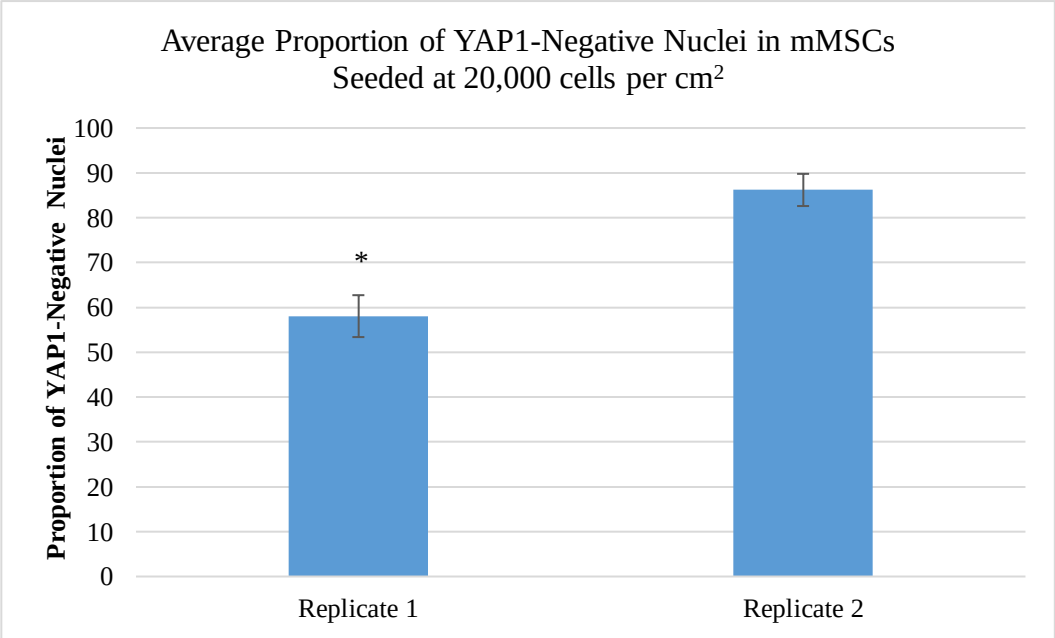

Figure 35 Average proportion of YAP1-negative nuclei in mMSCs seeded at 20,000 cells per cm^2 in replicate experiments. * indicates $p < 0.05$ compared to replicate 2.

Chapter 4

Conclusions and Future Work

In this project, mesenchymal stem cells were cultured at different time points, different densities, and on different substrates and analyzed for YAP1 localization to explore the effect of varied substrate architecture on YAP1 translocation and explain the role of YAP1 localization in the FAK/RhoA/YAP1 pathway that regulates osteogenic differentiation.

According to these experiments, cell density increases nuclear YAP1 localization and activation due to an increase in cell-cell contact inhibition. This YAP1 nuclear translocation is not temporally controlled but by cell-cell contacts alone. Data on the process of YAP1 translocation suggests that YAP1 may rapidly switch from the cytoplasm to the nucleus when a particular confluency is achieved rather than a gradual translocation process. The culturing on cells nanofiber surfaces compared to control flat surfaces revealed conflicting data on hMSC morphology in response to nanofibrous architecture. In general, cells adhered to nanofibers appeared more narrow and demonstrated less spreading than cells on flat surfaces. Nanofiber surfaces did increase nuclear YAP1 localization and focal adhesion size compared to control flat surfaces. Small nanofibers compared to medium and large nanofibers appeared to intensify the effect on YAP1 nuclear localization. Osteogenic differentiation was not shown to be different between hMSCs on nanofiber vs control surfaces but the effects on differentiation may have been limited by the relatively short 48-hour incubation.

Overall, these results begin to provide important information on the interactions of nanofibrous architecture and stem cells and the role of YAP1 in osteogenic differentiation. It is concluded that stem cell contact with nanofibrous architecture results in the formation of larger focal adhesions compared to a flat surface, which increases RhoA activity and thus RhoA-dependent YAP1 nuclear translocation. In the nucleus, YAP1 is able to regulate gene transcription potentially through the transcription factor Runx2.

Further experiments are necessary to conclude if nanofiber surfaces increase YAP1 nuclear localization to promote the FAK/RhoA/YAP1 pathway to osteogenic differentiation. Experiments on cell morphology of hMSCs grown on these substrates should be repeated to clarify which forms cells with a more in-vivo-like morphology. Experiments should also be completed to reveal the effects of nanofibrous architecture on FAK phosphorylation at 576/577, which could include immunofluorescence staining or western blots. Foremost, however, are additional experiments on osteogenic differentiation of hMSCs grown on nanofibers. Data from these experiments would be critical for uncovering the potential value of nanofibrous scaffolds in regulating bone homeostasis through the FAK/RhoA/YAP1 pathway. Any experiments observing osteogenic differentiation may be improved by the use of differentiation medium.

Understanding the FAK/RhoA/YAP1 pathway through modification of substrate architecture may aid in the development of biomaterials for tissue regeneration.

Appendix A

Experimental Data

Table 1 Proportion of mMSCs with cytoplasmic YAP1 localization at 24-hour, 72-hour, and 1-week time points.

Time Point	Total Nuclei	Total Negative Nuclei	Percent	Average	Standard Deviation	Average Density (cells/22 mm^2)
24 hours	754	514	68.17	65.21	17.68	120640
72 hours	2222	2108	94.87	94.21	4.43	355200
1 week	1396	1331	95.34	96.80	3.42	223360

Table 2 Time course p-values.

T-test	P-value
24 hr vs 72 hr	0.000493559
24 hr vs 1 week	0.000275974
72 hr vs 1 week	0.161459383

Table 3 Proportion of mMSCs with cytoplasmic YAP1 localization seeded at 10,000; 20,000; or 40,000 cells per cm^2.

Seeding Density	Total Nuclei	Total Negative Nuclei	Percent	Average	Standard Deviation
LowA (10K/cm^2)	390	295	75.64	56.08	29.80
MediumA (20K/cm^2)	289	171	59.17	58.06	15.49
HighA (40K/cm^2)	597	546	91.46	89.77	15.71

Table 4 Seeding density p-values.

T-test	P-value
LowA vs MediumA	0.847849662
LowA vs HighA	0.004636005
MediumA vs HighA	0.000117358
HighA vs 72 hr	0.387789975

Table 5 Proportion of mMSCs with cytoplasmic YAP1 localization seeded at 25,000; 30,000; or 35,000 cells per cm^2.

Seeding Density	Total Nuclei	Total Negative Nuclei	Percent	Average	Standard Deviation
LowB (25K/cm^2)	262	192	73.28	69.42	17.09
MediumB (30K/cm^2)	314	295	93.95	90.12	14.71
HighB (35K/cm^2)	374	357	95.45	94.51	5.08

Table 6 Seeding density p-values.

T-test	P-value
LowB vs MediumB	0.009642913
LowB vs HighB	0.00107654
MediumB vs HighB	0.390866057
MediumA vs LowB	0.128675336
HighB vs HighA	0.361598178

Table 7 Proportion of mMSCs with cytoplasmic YAP1 localization seeded at 20,000; 25,000; or 30,000 cells per cm^2.

Seeding Density	Total Nuclei	Total Negative Nuclei	Percent	Average	Standard Deviation
LowC (20K/cm2)	448	400	89.29	86.19	15.25
MediumC (25K/cm2)	615	518	84.23	72.15	22.63
HighC (30K/cm2)	469	429	91.47	87.52	16.11

Table 8 Averaged seeding density p-values.

T-test	P-value
10K vs 20K	0.066585157
20K vs 25K	0.427612906
25K vs 30K	0.000821493
30K vs 35K	0.076408109
35K vs 40K	0.361598178
10K vs 25K	0.145424769
10K vs 30K	0.004924238
10K vs 35K	0.001570333
10K vs 40K	0.004636005
40K vs 30K	0.814466692
40K vs 25K	0.005697968
40K vs 20K	0.027755093
35K vs 25K	3.2317E-06
20K vs 30K	0.009363383
20K vs 35K	5.24583E-05

Table 9 Average area, aspect ratio, circularity index, and nuclear YAP1 fluorescence intensity of hMSCs seeded on 10% PMMA nanofibers or a control flat surface.

	10% PMMA NF	**CS**
Average Area in μm^2	1407.11	3004.48
Standard Error	125.09	298.99
Average Aspect Ratio	5.45	2.24
Standard Error	0.34	0.13
Average Circularity Index	0.11	0.17
Standard Error	0.01	0.03
Average nuclear YAP1 fluorescence intensity	274.12	186.71
Standard Error	15.19	8.56

Table 10 T-test values for area, aspect ratio, circularity index, and nuclear YAP1 fluorescence intensity between hMSCs seeded on 10% PMMA nanofibers or a control flat surface.

T-test	**P-value**
Area	1.91048E-06
Aspect Ratio	7.19593E-17
Circularity Index	0.046613127
Nuclear YAP1 fluorescence intensity	1.01953E-06

Table 11 Average area, aspect ratio, circularity index, and vinculin patch area of hMSCs seeded on 10% PMMA nanofibers or a control flat surface.

	10% PMMA NF	**CS**
Average Area in μm^2	816.76	3904.01
Standard Error	49.63	230.49
Average Aspect Ratio	7.25	3.02
Standard Error	0.51	0.12
Average Circularity Index	0.15	0.06
Standard Error	0.01	0.00
Average vinculin patch area in μm^2	2.56	2.25
Standard Error	0.13	0.05

Table 12 T-test values for area, aspect ratio, circularity index, and vinculin patch area between hMSCs seeded on 10% PMMA nanofibers or a control flat surface.

T-test	P-value
Area	1.52395E-29
Aspect ratio	5.33684E-14
Circularity index	4.9104E-14
Average vinculin patch area	1.55948E-25

Table 13 Average nuclear YAP1 fluorescence intensity of hMSCs seeded on 3, 6.5, or 10% PMMA nanofibers or a control flat surface.

	CS	3% PMMA NF	6.5% PMMA NF	10% PMMA NF
Average nuclear YAP1 fluorescence intensity	326.75	1286.86	447.18	462.98
Standard Error	12.16	93.51	20.75	22.38

Table 14 Different size nanofiber substrates and control flat surface p-values.

T-test	P-value
CS vs 3% PMMA NF	3.31801E-18
CS vs 6.5% PMMA NF	1.39777E-06
CS vs 10% PMMA NF	5.57377E-07
3% PMMA NF vs 6.5% PMMA NF	6.59883E-15
3% PMMA NF vs 10% PMMA NF	1.88826E-14
6.5% PMMA NF vs 10% PMMA NF	0.60547454

Table 15 Average alkaline phosphatase activity of hMSCs seeded on 10% PMMA nanofibers or a control flat surface and p-value.

	10% PMMA NF	CS
Average	5.87	5.09
Standard Error	0.63	0.65
T-test p-value	0.424	

BIBLIOGRAPHY

Chang, B., Ma, C., & Liu, X. (2018). Nanofibers Regulate Single Bone Marrow Stem Cell Osteogenesis via FAK/RhoA/YAP1 Pathway. *ACS Applied Materials & Interfaces,10*(39), 33022-33031. doi:10.1021/acsami.8b11449

Das, A., Fischer, R. S., Pan, D., & Waterman, C. M. (2016). YAP Nuclear Localization in the Absence of Cell-Cell Contact Is Mediated by a Filamentous Actin-dependent, Myosin II- and Phospho-YAP-independent Pathway during Extracellular Matrix Mechanosensing. *Journal of Biological Chemistry,291*(12), 6096-6110. doi:10.1074/jbc.m115.708313

Driscoll, T., Cosgrove, B., Heo, S., Shurden, Z., & Mauck, R. (2015). Cytoskeletal to Nuclear Strain Transfer Regulates YAP Signaling in Mesenchymal Stem Cells. *Biophysical Journal,108*(12), 2783-2793. doi:10.1016/j.bpj.2015.05.010

Elosegui-Artola, A., Andreu, I., Beedle, A., Lezamiz, A., Uroz, M., Kosmalska, A. J., . . . Roca-Cusachs, P. (2017). Force Triggers YAP Nuclear Entry by Regulating Transport across Nuclear Pores. *Cell,171*(6), 1397-1410. doi: 10.1016/j.cell.2017.10.008

Nardone, G., Oliver-De La Cruz, J., Vrbsky, J., Martini, C., Pribyl, J., Skládal, P., . . . Forte, G. (2017). YAP regulates cell mechanics by controlling focal adhesion assembly. *Nature Communications,8*. doi:10.1038/ncomms15321

Piperno, S., Lozzi, L., Rastelli, R., Passacantando, M., & Santucci, S. (2006). PMMA nanofibers production by electrospinning. *Applied Surface Science,252*, 5583-5586. doi:10.1016/j.apsusc.2005.12.142

Pirone, D. M., Liu, W. F., Ruiz, S. A., Gao, L., Raghavan, S., Lemmon, C. A., . . . Chen, C. S. (2006). An inhibitory role for FAK in regulating proliferation: A link between limited adhesion and RhoA-ROCK signaling. *The Journal of Cell Biology,174*(2), 277-288. doi:10.1083/jcb.200510062

Sheets, K., Wunsch, S., Ng, C., & Nain, A. S. (2013). Shape-dependent cell migration and focal adhesion organization on suspended and aligned nanofiber scaffolds. *Acta Biomaterialia,9*(7), 7169-7177. doi:10.1016/j.actbio.2013.03.042

Vasita, R., & Katti, D. S. (2006). Nanofibers and their applications in tissue engineering. *International Journal of Nanomedicine,1*(1), 15-30. doi:10.2147/nano.2006.1.1.15

What is the Hippo-YAP/TAZ tumor-suppressor pathway? by the National University of Singapore is licensed under CC BY-NC 4.0. Retrieved from https://www.mechanobio.info/what-is-mechanosignaling/signaling-pathways/what-is-the-hippo-yaptaz-tumor-suppressor-pathway/

Zhang, H., Cooper, L. F., Zhang, X., Zhang, Y., Deng, F., Song, J., & Yang, S. (2016). Titanium nanotubes induce osteogenic differentiation through the FAK/RhoA/YAP cascade. *RSC Advances,6*(50), 44062-44069. doi:10.1039/c6ra04002k

Zhao, B., Wei, X., Li, W., Udan, R. S., Yang, Q., Kim, J., . . . Guan, K. (2007). Inactivation of YAP oncoprotein by the Hippo pathway is involved in cell contact inhibition and tissue growth control. *Genes & Development,21,* 2747-2761. doi:10.1101/gad.1602907

Academic Vita

Coreena Chan

EDUCATION

The Pennsylvania State University University Park, PA August 2015 – May 2019
Schreyer Honors College – Honors in Biology
Bachelor of Science: Biology (Neuroscience Focus), Sociology Minor

RESEARCH EXPERIENCE

Musculoskeletal Regenerative Engineering Laboratory – Brown Lab
- University Park, PA December 2016 – May 2019
- *Undergraduate Researcher at Penn State University*

Neural and Behavioral Sciences Laboratory – Silberman Lab
- Hershey, PA Summer 2018
- *Undergraduate Research Assistant at Penn State College of Medicine*

Center for Neuroscience Summer Undergraduate Research Program (SURP) – Torregrossa Lab
- Pittsburgh, PA Summer 2017
- *Undergraduate Research Fellow at University of Pittsburgh*

ACTIVITIES AND INVOLVEMENT

Penn State BIOL 469: Neurobiology
- University Park, PA August 2018 – December 2018
- *Undergraduate Teaching Assistant*

Penn State Health Milton S. Hershey Medical Center
- Hershey, PA May 2018 – March 2019
- *Patient Experience Volunteer*

Mid Central Pennsylvania Red Cross Chapter
- State College, PA September 2017 – May 2019
- *Hours Manager and Blood Drive On-site Coordinator*

Schreyer Honors College Career Development Program
- University Park, PA October 2017 – May 2018
- *Undergraduate Mentor*

The GLOBE
- University Park, PA August 2015 – May 2017
- *Resident Member*

HONORS AND AWARDS

Valedictorian – Central York High School in York, Pennsylvania
Dean's List (Fall 2015, Spring 2016, Fall 2016, Spring 2017, Fall 2017, Spring 2018, Fall 2018)
Scholarship Awards
- Doris N. McKinstry Scholarship – awarded to an outstanding female undergraduate biology student in Eberly College of Science
- Academic Excellence Scholarship – awarded to Schreyer Scholars maintaining good academic standing
- Schumacher Honors Scholarship – awarded in recognition of academic accomplishments by Schreyer Honors College
- Prystowsky Trustee Scholarship – awarded for exceptional promise for success and academic achievement by Eberly College of Science
- Jimmy Rane Foundation Scholarship – awarded for academic excellence, leadership skills, community involvement, and awards/honors
- JLY Sustainers' Scholarship – awarded to a woman with demonstrated exceptional dedication to volunteerism by the Junior League of York